

# Physical and mechanical properties and thermal protection efficiency of intumescent coatings

V G Zverev<sup>1</sup>, V I Zinchenko<sup>1</sup> and A F Tsimbalyuk<sup>2</sup>

<sup>1</sup> Tomsk State University, 36, Lenina ave., Tomsk, 634050, Russia

<sup>2</sup> Tomsk Polytechnic University, 30, Lenina ave., Tomsk, 634050, Russia

E-mail: zverev@niipmm.tsu.ru

**Abstract.** The new engineering technique for the experimental investigation of physical and mechanical characteristics of thermal protective intumescent coatings is offered. A mathematical model is proposed for predicting the thermal behavior of structures protected by coatings; the model is closed by the studied material characteristics. The heating of a metal plate under standard thermal loading conditions is modeled mathematically. The modeling results are in good agreement with bench test results for metal temperature under the coating. The proposed technique of studying physical and mechanical characteristics can be applied to identify and monitor the state of thermal protective intumescent coatings in the long-term operation.

## 1. Introduction

The wide application of structural materials requires the improvement of their stability under extreme thermal loading of various origin, intensity and duration, particularly, in industrial fires [1]. Today there is a broad range of materials and compositions for passive thermal protection [2]. Intumescent paint coatings have great potential in this regard.

A 1 ÷ 2 mm thick layer of intumescent coating retains the thermal stability of the substrate for up to 1 ÷ 1.5 h. The protective properties of intumescent coatings are due to a considerable increase of their thickness upon heating. The char produced during intumescence has low porosity, low thermal conductivity and serves as a protective barrier between the substrate and high-enthalpy gaseous medium. This greatly increases thermal resistance, but significantly reduces heat flux to the substrate [3, 4]. Modern intumescent coatings have an expansion ratio of up to 20...40, char porosity amounts to ~ 0.95...0.98, density is ~ 30...50 kg/m<sup>3</sup>, and thermal conductivity coefficient is ~ 0.04...0.1 W/(m·K) [1].

Intumescent coatings are of practical interest as they have minimum weight and thickness per unit of protected area, high heat insulating properties of char, and can be deposited by industrial methods. Currently, requirements for the thermal protection of structures have increased. This necessitates the development and application of new, more effective universal materials with high adhesion to any surfaces that are able to resist vibration and weather.

To expand the applications of intumescent coatings, we must investigate their physical and mechanical properties, conduct laboratory and bench-scale studies, develop mathematical models to predict the state of structures and optimize their thermal protection under thermal conditions.



The paper is aimed to develop an engineering technique for studying the physical and mechanical properties of intumescent coatings and to apply a mathematical model for structure stability prediction under extreme thermal conditions.

## 2. Physical and mechanical properties of intumescent coatings under isothermal heating

Intumescent coatings are usually multicomponent compositions because many practically important factors are needed for their operation, such as adhesion, gas generation, intumescence, char strength and so on. The physical and chemical processes that accompany intumescence as well as formulations of used compositions are very diverse and often unknown. At the same time, intumescent coatings exhibit a common feature associated with thickness (volume) increase during heating. Their study must therefore be based on the characteristics that integrally characterize intumescence and can be adequately determined in a simple laboratory experiment. This would make possible the control of the coating state during the operation. These characteristics are the expansion ratio due to intumescence and the mass of the intumescent coating sample during isothermal heating.

The characteristics were determined using a technique based on the method of thermally stabilized states of the material. The experimental procedure is schematically shown in Figure 1. Samples presented a two-layer coating–substrate system with the initial coating thickness of  $\sim 2$  mm. They were placed into thermally stable glass tubes of  $\sim 17.5$  mm in diameter with a flat bottom. The substrate was used in the experiment in order to model the coating operation in real conditions.

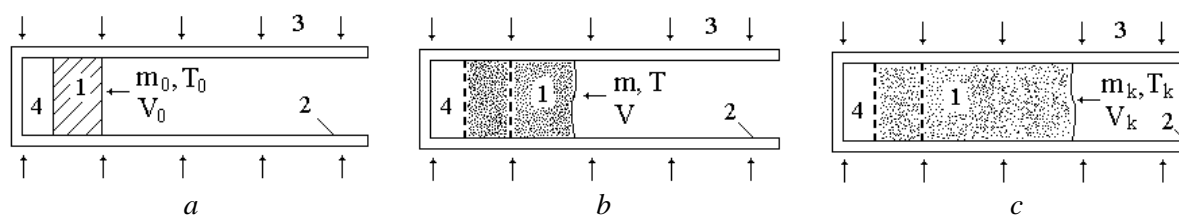


**Figure 1.** Schematics of the experiment, and various physical and mechanical states of a sample on the substrate during thermostating. *a* – initial (subscript 0), *b* – current, *c* – final (subscript *k*) state (at high temperatures). *m* – mass, *T* – temperature, *V* – sample volume; 1 – sample (an intumescent layer), 2 – thermally stable glass tube, 3 – heat flux, 4 – substrate.

Then the samples were kept for  $\sim 20$  min in a muffle furnace in inert gas (nitrogen) atmosphere at given thermostating temperature *T* that was maintained automatically with an error of  $\pm 5$  K. The temperature range was from 300 to 900 K with step 25; 50 K. Thermal loading causes changes in the state of the intumescent coating in both its volume and mass. Since the material expands in one direction along the tube, the volume change can be easily determined by the coating sample thickness. To exclude random factors and to define confidence error intervals for measurement results, 3 to 5 samples were kept at the same temperature.

In experiments the initial coating thickness varied from 1 to 6 mm, and the diameter varied from 6 to 40 mm. It was found that relative volume and mass changes in isothermally heated samples do not depend on their initial thickness and diameter, which is in accordance with the notion of elementary material volume and the physical nature of intumescence.

Different coating states were observed depending on thermostating temperature. At  $T \sim 170$  °C the volume changed by a factor of  $\sim 8$  with a dense layer structure. At higher temperatures  $T > 300$  °C the volume changed by a factor of more than 20 with the formation of a loose char structure in the form of elongated intumescent fibers. Thus, each thermostating temperature is characterized by a particular volume, structure and mass of the sample material, which corresponds to quasi-equilibrium processes of intumescence and thermal decomposition.

Upon thermostating we weighed (with an error of  $\sim 10^{-6}$  kg) and measured ( $\sim 10^{-4}$  m) the samples, determined their mass *m* and length (thickness) *h*, and calculated relative quantities

$$dm = m_0 - m, \quad dh = h - h_0, \quad \bar{m} = m / m_0, \quad \theta = dh / h_0,$$

where subscript 0 corresponds to the initial state, and  $\theta$  is the expansion ratio. Density of char  $\rho$  and porosity of char  $\varphi_g$  were calculated by formulas

$$\rho = \frac{\rho_0(m/m_0)}{1 + \theta}, \quad \varphi_g = 1 - \frac{(m/m_0)}{1 + \theta}. \quad (1)$$

We ignored initial porosity in the formula for  $\varphi_g$ , assuming that the true char porosity coincides with the initial one. Thus, porosity in equation (1) is fully determined by the loss of mass of the solid material and its intumescence. The set of the discussed physical and mechanical characteristics ( $\theta$ ,  $m/m_0$ ) individually characterizes the intumescent coating and can be considered as the material response to a thermodynamic state change. This set is necessary for the mathematical modeling of coating heating and for the coating state monitoring during a long-term operation on structures.

Figure 2 displays experimental data for the discussed characteristics of two coatings SGK-2 [5] and SGK-1 [1] depending on thermostating temperature. These coatings differ in composition and a binder-to-filler ratio. Figure 2a demonstrates that intumescence of SGK-2 occurs in two stages: the first stage corresponds to  $400 \text{ K} < T < 600 \text{ K}$ , the second stage corresponds to  $600 \text{ K} < T < 800 \text{ K}$ . Then the equilibrium curve of the expansion ratio approaches an asymptote with value  $\sim 24 \div 25$ . Initial coating intumescence is drastic and occurs later than that of SGK-1. The height of the first plateau is  $\theta \sim 16$  ( $\sim 10$  for SGK-1), which is advantageous of this composition because heat transfer in this case is suppressed more efficiently at low temperatures.

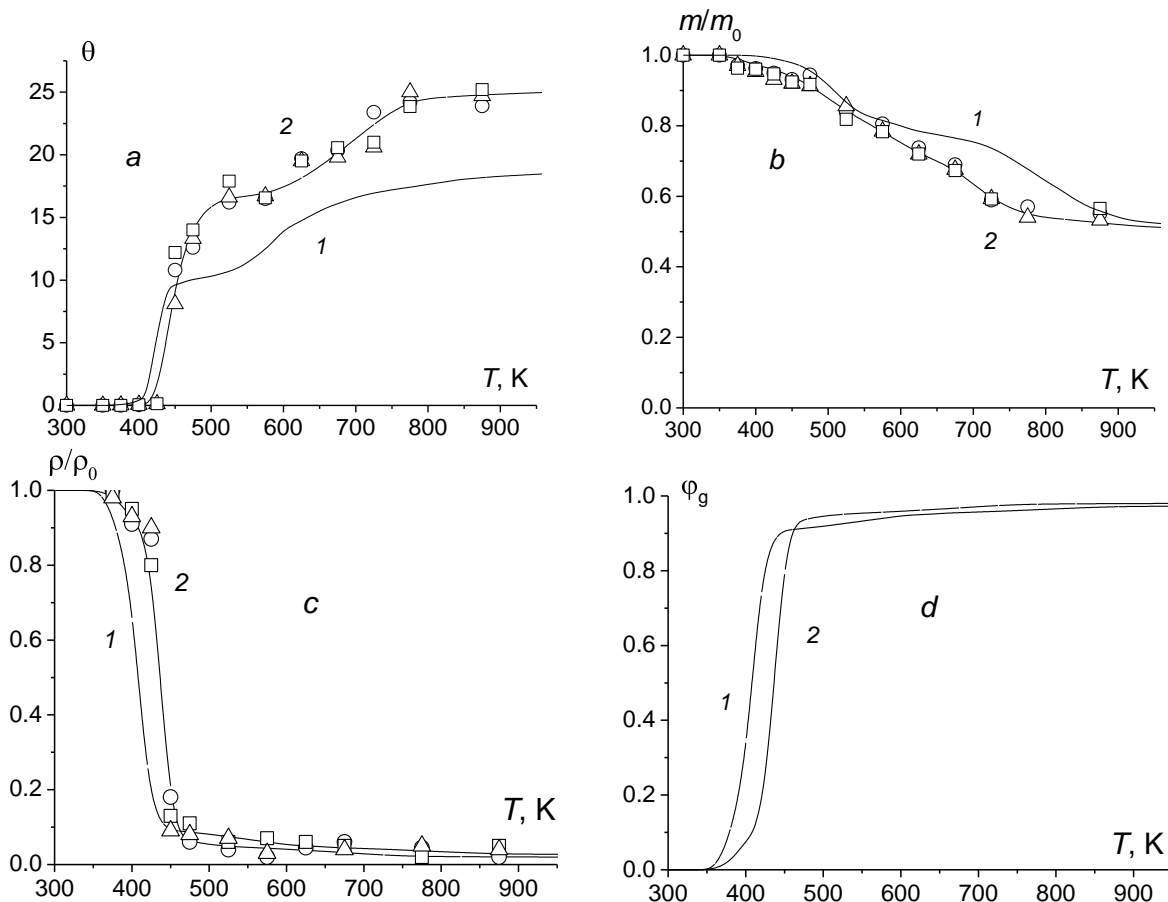


**Figure 2.** Expansion ratio (a), mass (b), density (c), porosity (d) of coating samples vs. temperature.

1 – SGK-1; 2 – SGK-2;  $\Delta$ ,  $\square$ ,  $\circ$  – experimental data.

According to Figure 2b, the loss of mass of coating SGK-2 within the temperature range of 400 K <  $T$  < 800 K is slightly larger than for SGK-1. The final output of char is nevertheless almost similar, being  $\sim 0.52$ . The wave-like shape of curve 2 indicates that thermal destruction of the coating occurs in several stages. Notice that intumescence prevails over the release of gaseous products at the initial stage for both coatings. For example, at  $T \sim 450$  K and 4...5 % of mass loss the layer thickness increases by a factor of  $\sim 14$ . This is the main mechanism for the formation of thermal protection properties of the coating.

As one can see from Figure 2c, the SGK-2 coating density changes by a factor of more than 12 at the first intumescence stage and by a factor of only 2 at the second stage. At  $T \sim 900$  K the char density approaches  $\rho \sim 20$  kg/m<sup>3</sup>. Peeling of density curves 1 and 2 is observed within the range of  $T \sim 375 \div 450$  K. At the same mass loss (< 5 %) for these materials this is related to the delay of the SGK-2 intumescence curve by the temperature. Curves 1 and 2 of porosity  $\phi_g$  increase abruptly up to  $\sim 0.9$  at the first intumescence stage (Figure 2d). The final porosity value for coating SGK-2 is  $\phi_g \sim 0.98$ .

The considered characteristics provide information about the state and structure of the intumescent coating layer; they allow us to compare with the same characteristics of other intumescent coatings and to evaluate their thermal protection properties. The expansion ratio increase up to  $\theta \sim 25$  is a definite advantage of the SGK-2 composition. The layer thickness strongly affects the thermal protection capacity of the coating during non-stationary heat transfer because the characteristic heating time depends quadratically on this parameter. However, there is no point in further intumescence as it enhances radiation heat transfer in the porous medium and may lead to damage of a char structure due to its strength reduction.

## 2. Mathematical modeling of intumescent coating heating

Thermal processes in the coating layer will be considered in the framework of a mathematical non-stationary heat transfer model [6, 7]. The model can be applied to a broad range of coatings as it has been proved to be good for practical calculations [8]. The schematic layout of layers and coordinate system are given in Figure 3a. The initial coating thickness is  $h_0$ , and that of the substrate is  $h_b$ . The intumescent coating will be considered as a porous two-phase, one-temperature medium that contains a solid and gaseous phase. We assume that the material expands in one dimension and does not shrink due to a chemical or mechanical interaction with the heated gaseous medium, which corresponds to the real process.

Without going into details of the intumescence and thermal destruction mechanisms, we determine relative mass and volume changes in an elementary intumescent coating sample through  $\bar{m} = m/m_0$  and  $\bar{\theta} = V/V_0 = 1 + \theta$ . Along with the Euler coordinate system ( $x$ ), the Lagrangian coordinate system ( $s$ ) related to the char material will be used.

Using the laws of conservation of mass and energy, the following system of equations is obtained in the Lagrangian coordinate system ( $t, s$ ) [6]:

$$\rho_0 \frac{\partial \bar{m}}{\partial t} + \frac{\partial G_g}{\partial s} = 0, \quad 0 \leq s \leq h_0, \quad x = h_b + \int_0^s \bar{\theta} ds, \quad (2)$$

$$(\rho c_p)_{ef} \bar{\theta} \frac{\partial T}{\partial t} + (c_p G)_g \frac{\partial T}{\partial s} = \frac{\partial}{\partial s} \left( \frac{\lambda_{ef}}{\bar{\theta}} \frac{\partial T}{\partial s} \right) + \rho_0 Q \frac{\partial \bar{m}}{\partial t}, \quad (3)$$

$$\frac{\partial \bar{m}}{\partial t} = -R_s(T, \bar{m}), \quad (4)$$

$$(\rho c_p)_{ef} = (\rho c_p)_s \phi_s + (\rho c_p)_g \phi_g, \quad \phi_s + \phi_g = 1, \quad (5)$$

$$\lambda_{ef} = \lambda_s \phi_s + \lambda_g \phi_g + \lambda_r \phi_g, \quad \lambda_r = 4\epsilon_{ss} \sigma d_p \bar{\theta}^{-1/3} T^3.$$

The substrate state is described by the thermal conductivity equation for inert materials:

$$(\rho c_p)_b \frac{\partial T}{\partial t} = \frac{\partial}{\partial x} \left( \lambda_b \frac{\partial T}{\partial x} \right), \quad 0 < x < h_b. \quad (6)$$

The boundary conditions for equations (2), (3) and (6) read:

$$x = 0: \quad \lambda_b \frac{\partial T}{\partial x} = 0. \quad (7)$$

$$x = h_b, \quad s = 0: \quad \lambda_b \frac{\partial T}{\partial x} = \frac{\lambda_{ef}}{\theta} \frac{\partial T}{\partial s}, \quad T|_{x=h_b} = T|_{s=0}, \quad G_g = 0. \quad (8)$$

$$s = h_0: \quad \frac{\lambda_{ef}}{\theta} \frac{\partial T}{\partial s} = \alpha_f (T_f(t) - T_w) + \varepsilon_{fw} \sigma (T_f^4(t) - T^4). \quad (9)$$

$$T_f(t) - T_0 = 345 \lg(0.133t + 1), \quad \varepsilon_{fw} = [1 + (\bar{\varepsilon}_w^{-1} - 1) + (\bar{\varepsilon}_f^{-1} - 1)]^{-1}. \quad (10)$$

The initial conditions for equations (2)–(4) and (7) correspond to thermal equilibrium:

$$t = 0: \quad T = T_0, \quad \bar{m} = 1, \quad \bar{\theta} = 1, \quad s = x - h_b. \quad (11)$$

Here,  $t$  is the time,  $G_g$  is the filtration gas flow,  $\rho$ ,  $c_p$ ,  $\lambda$  are the density, specific heat capacity and thermal conductivity coefficient,  $Q$ ,  $R_s$  are the thermal effect and rate of thermal coating destruction,  $\varphi$  is the volume fraction of phase,  $\alpha$  is the heat transfer coefficient,  $\varepsilon$ ,  $\sigma$  are the emissivity factor and Stefan–Boltzmann constant, and  $d_p$  is the initial pore diameter. Subscripts  $s$ ,  $g$  are the solid and gaseous phases of char,  $w$  is the coating surface,  $f$  is the high-enthalpy gaseous medium (fire),  $r$  is the radiation,  $b$  is the substrate, 0 are the initial and  $ef$  are the effective values.

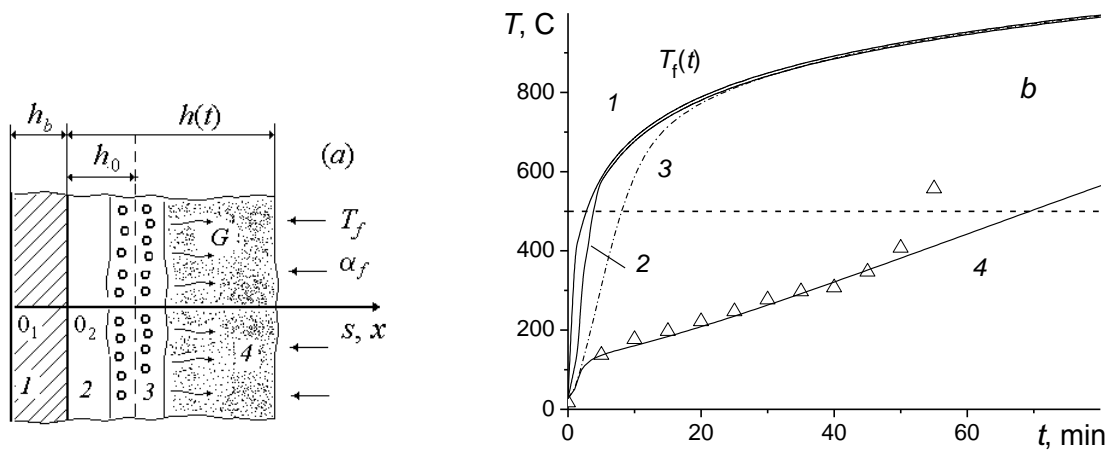


**Figure 3.** Schematic layout of layers (a) and calculation results on heating (b) of metal substrate with coating SGK-2 in standard fire.  $h_b = 5$  mm,  $h_0 = 2.2$  m. a: 1 – substrate; 2 – initial material; 3 – intumescence zone; 4 – char;  $h_0$ ,  $h(t)$  – initial, current layer thickness;  $G$  – filtration gas flow; b: 1 –  $T_f(t)$ , fire temperature; 2 –  $T_w(t)$ , coating surface temperature; 3, 4 – uncoated and coated metal temperature;  $\Delta$  – experimental data.

Equations (2) and (4) are the law of conservation of mass for the intumescent coating as a whole and for its solid phase; equation (3) is the energy equation with regard to filtration of gaseous decomposition products. Expressions (5) define the thermophysical properties of the porous medium and radiant thermal conductivity in pores [1]. The back side of the substrate is perfectly thermally isolated (equation (7)); the coating–substrate interface is under the conjugate conditions (equation (8)). The coating surface is under the radiative-convective effect of “standard” fire (equation (9)) which

temperature changes according to law (10) [9]. The model was closed by defining parameters  $\bar{m}$ ,  $\bar{\theta}$  [6].

### 3. Calculation results and their analysis

Figure 3b shows the calculation results obtained with mathematical model (2)–(11) on the thermal behavior of a 5-mm thick steel plate protected by a 2.2-mm thick layer of coating SGK-2 thermally loaded by standard fire (10) [9]. The coordinate of intersection of curves 3 and 4 with horizontal  $T = 500^\circ\text{C}$  (critical temperature for steel, a dashed line) gives the fire resistance time of the plate.

It is seen that a relatively thick, but unprotected metal layer cannot resist fire for more than 8 min (curve 3). The mathematically calculated estimates show that the deposition of a 2.2-mm thick SGK-2 coating increases the fire resistance time up to almost 70 min (curve 4), which greatly exceeds the practically important fire resistance time limit of one hour. As it follows from the figure, our calculation results and the experimental data of fire tests performed according to fire safety standards show a good agreement up until 50 minutes. The subsequent difference is due to partial spallation of surface char layers in the experiment, which was not taken into account in the mathematical model.

### 4. Conclusion

1. An original engineering technique is proposed for studying the physical and mechanical characteristics of thermal protective intumescent coatings. It is based on the determination of an expansion ratio and the mass loss of the coating sample under isothermal heating.

2. The technique can be applied to solve problems of identifying and monitoring the state of intumescent coatings during the operation.

3. The obtained coating characteristics are used to mathematically model the heating of a steel plate coated with SGK-2 and to demonstrate a high thermal protection efficiency of the coating. The modeling results agree well with bench test results.

4. The studied physical and mechanical characteristics of coating SGK-2 as well as the proposed mathematical model can be applied to optimize and improve the protection of structures against extreme thermal loading of various intensity and duration.

The work was supported by Project No. 9.1024.2014/K of the RF Ministry of Education and Science.

### Reference

- [1] Strakhov V L, Krutov A M and Davydkin N F 2000 *Fire Protection of Engineering Structures* (Moscow. Information and Publishing Centre 'TIMR')
- [2] Sobur S V 2003 *Fire protection of materials and structures Handbook* (Moscow. Spetsstekhnika Publ.)
- [3] Griffin G J 2010 *J. of Fire Science* **28** 249
- [4] Bartholmai M, Schriever R and Scharfel B 2003 *Fire and Materials* **27** 151
- [5] TU 7719-171-21366107-02 2002 *Fire-retardant intumescent composition SGK-2* (Moscow. Spetsenergetekhnika Publ.)
- [6] Zverev V G, Nesmelov V V, Tsimbalyuk A F and Gol'din V D 1998 *Combustion, Explosion and Shock Waves* **34** 198
- [7] Anderson Jr. C E, Wauters D K 1984 *International Journal of Engineering Science* **22** 881
- [8] Zverev V G, Nazarenko V A and Tsimbalyuk A F 2008 *High Temperatures* **46** 254
- [9] Drysdale D 1985 *An Introduction to Fire Dynamics* (Chichester: John Wiley and Sons)